

Isolation of a Bimetallic Cobalt(III) Nitride and Examination of Its Hydrogen Atom Abstraction Chemistry and Reactivity Towards H₂

Debabrata Sengupta,[†] Christian Sandoval-Pauker,[‡] Emily Schueller,[#] Angela Marisol Encerrado-Manriquez,[†] Alejandro Metta-Magaña,[†] Wen-Yee Lee,[†] Ram Seshadri,^{#,Δ} Balazs Pinter,^{*,‡} and Skye Fortier^{*,†}

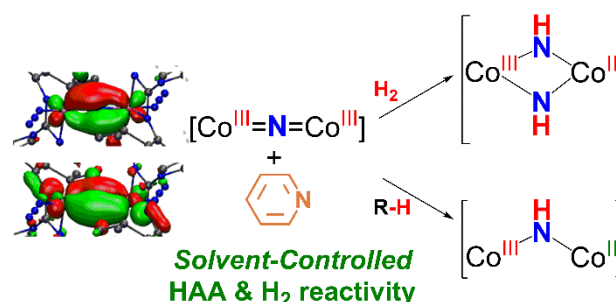
[†]Department of Chemistry and Biochemistry, University of Texas at El Paso, El Paso, Texas 79968, United States

[‡]Department of Chemistry, Universidad Técnica Federico Santa María, Valparaíso, 2390123, Chile

[#]Materials Department and Materials Research Laboratory, University of California, Santa Barbara, California 93106, United States

^ΔDepartment of Chemistry and Biochemistry, University of California, Santa Barbara, California 93106, United States

ABSTRACT: Room temperature photolysis of the bis(azide)cobaltate(II) complex [Na(THF)_x][(ket-guan)Co(N₃)₂] (ket-guan = [(^tBuCN)C(NDipp)₂][−], Dipp = 2,6-diisopropylphenyl) (**3a**) in THF cleanly forms the binuclear cobalt nitride [Na(THF)₄][(ket-guan)Co(N₃)₂(μ-N)]_n (**1**). Compound **1** represents the first example of an isolable, bimetallic cobalt nitride complex, and it has been fully characterized by spectroscopic, magnetic, and computational analyses. Density functional theory supports a Co^{III}=N=Co^{III} canonical form with significant π-bonding between the cobalt centers and the nitride atom. Unlike other Group 9 bridging nitride complexes, no radical character is detected at the bridging N-atom of **1**. Indeed, **1** is unreactive towards weak C-H donors and even co-crystallizes with a molecule of cyclohexadiene (CHD) in its crystallographic unit cell to give **1**·CHD as a room temperature stable product. Notably, addition of pyridine to **1** or photolyzed solutions of [(ket-guan)Co(N₃)(py)]₂ (**4a**) leads to destabilization via activation of the nitride unit, resulting in the mixed-valent Co(II)/(III) bridged imido species [(ket-guan)Co]₂(μ-NH)(μ-N₃) (**5**) formed from intermolecular hydrogen atom abstraction (HAA) of strong C-H bonds (BDE ~ 100 kcal/mol). Kinetic rate analysis of the formation of **5** in the presence of C₆H₁₂ or C₆D₁₂ gives a KIE = 2.5±0.1, supportive of a HAA formation pathway. The reactivity of our system was further probed by photolyzing C₆D₆/py-*d*₅ solutions of **4a** under an H₂ atmosphere (150 psi), which leads to the exclusive formation of the bis(imido) [(ket-guan)Co(μ-NH)]₂ (**6**) as a result of dihydrogen activation. These results provide unique insights into the chemistry and electronic structure of late 3d-metal nitrides while providing entryway into C-H activation pathways.



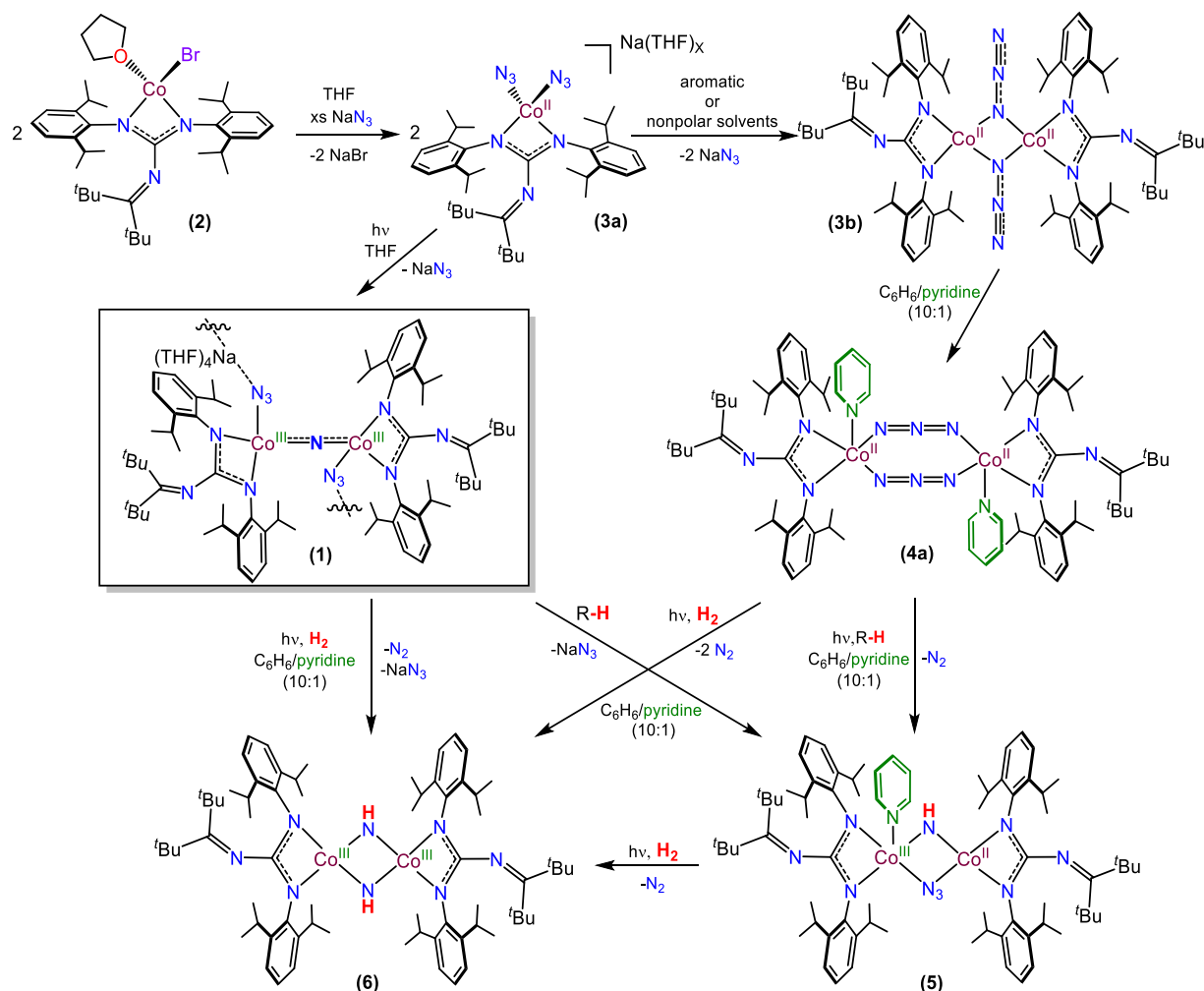
INTRODUCTION

Complexes containing metal-ligand multiple bonds, both biological and synthetic, have been intensively investigated owing to the participation of these moieties in a host of important reactions including C-H bond activation,¹ olefin metathesis,² cycloaddition,³ and heteroatom transfer reactivity.⁴ Indeed, the Fe=O intermediate formed in the active site of cytochrome P450 is critical for its enzymatic versatility.⁵ Of note, isolable compounds containing M=E or M≡E bonds have been dominated by the early to mid-transition metals, while the synthesis and isolation of late metal complexes presents a more significant challenge due to the progressive population of M=E/M≡E π*-orbitals, leading to high reactivity and instability.⁶⁻⁸

In specific regard to Group 9 – 11 metals in tetragonal ligand fields, it is considered the case that *d*-orbital occupation with electron counts of *n* ≥ 4 is incompatible with metal-ligand multiple bonds, a concept that has been coined the “oxo

wall.”^{9, 10} Yet, the oxo wall can be circumvented through lowering the coordination number and symmetry, employing sterically encumbering ligands,^{7, 11-12} and reducing the *d*-electron count through metal oxidation.^{6, 8, 13} These strategies have been effective for a handful of Rh/Ir compounds such as the iridium(V)oxo Ir(O)(mes)₃ (mes = mesityl) synthesized by Wilkinson,¹⁴ and nitride species such as (PNP)Ir(N) (PNP = N(CHCHP^tBu)₂) reported by the groups of de Bruin and Schneider,⁸ amongst others.¹⁵⁻¹⁹ However, this can lead to non-trivial canonical forms, which complicates electronic structure interpretations and formal oxidation state assignments.^{8, 20}

Extension of these synthetic strategies to cobalt has afforded a number of imido-complexes¹³ and recently led to the isolation and structural characterization of the first terminal cobalt(III)-oxo species [PhB(^tBuIm)₃]Co(O) (Im = imidazol-2-ylidene).²¹ Notably, though, terminal cobalt-nitrides still remain elusive. In 2010, Chirik et al. reported that thermolysis or photolysis of (ⁱPrPDI)CoN₃ (ⁱPrPDI = 2,6-(2,6-ⁱPr₂-C₆H₃-



Scheme 1. Synthetic overview and HAA reactivity with alkanes and H₂.

N=CMe)₂C₅H₃N) leads to intramolecular *N*-atom insertion, attributed to the formation of a fleeting terminal cobalt nitride.²² Later, Meyer and co-workers were able to trap an intermediate nitride complex through the use of the bis(*N*-heterocyclic carbene)-mono(phenolate) chelated compound (BIMPN^{Mes,Ad,Me})Co(N) at 10 K, which upon warming undergoes *N*-atom insertion into a Co-C bond.²³ Consequently, controlled reactivity studies of the cobalt-nitride moiety remain unknown.

It has come to light in recent years that the lifetime of Co=O complexes can be extended through the coordination of redox-inactive Lewis acids to the oxo moiety.²⁴ These compounds are still short-lived, but under this cooperative model, the second metal can alleviate charge density that would otherwise occupy antibonding orbitals, thereby extending lifetimes. Notably, Tomson and co-workers have capitalized upon this strategy utilizing macrocyclic pyridyl-diimine ligands to generate the putative dinuclear cobalt nitride [(^tPDI₂)Co₂(μ-N)(PMe₃)₂]³⁺.²⁵ This nitride is not observed but its formation is indicated through the isolation of phosphinimide and intramolecular C-H amination products formed as the result of passing Co-N-Co formation. Building upon this approach of utilizing bimetallic systems to stabilize Group 9 metal-ligand multiple bonds, we have targeted the synthesis of isolable homobimetallic bridging Co=N=Co complexes through steric and geo-

metric control to gain access and insight into elusive cobalt-nitride bonds.

As part of our ongoing effort to utilize bulky guanidinate ligands to stabilize 3d-metal complexes with rare and reactive bonding motifs,²⁶⁻²⁷ herein, we demonstrate the isolation and the reactivity studies of a mid-valent, four-coordinate, bimetallic Co(III)-nitride complex, namely {[Na(THF)₄][(ket^{guan})Co(μ-N)(N₃)₂]_n} (**1**) (ket^{guan} = (tBu₂CN)C(NDipp)₂, Dipp = 2,6-diisopropylphenyl). While **1** is stable as a solid and in solution, chemical activation of the nitride moiety can be achieved by perturbation of the ligand field through a coordination switch attained by simple addition of pyridine, resulting in intermolecular hydrogen atom abstraction (HAA) chemistry. Impressively, **1** can perform HAA on strong, unactivated C-H bonds (BDE ~ 100 kcal/mol), generating the parent-imido, mixed-valent complex [(ket^{guan})Co]₂(μ-NH)(μ-N₃) (**5**). Moreover, **1** is reactive towards dihydrogen, cleaving the H₂ bond (BDE ~ 105 kcal/mol) to give the bis(imido) [(ket^{guan})Co^{III}(μ-NH)]₂ (**6**).

The combined stability of **1** and its solvent-triggered nitride activation provides a unique platform and opportunity to study the chemistry of cobalt-nitrides and multiply bonded late 3d-metal complexes that lie beyond the oxo wall.

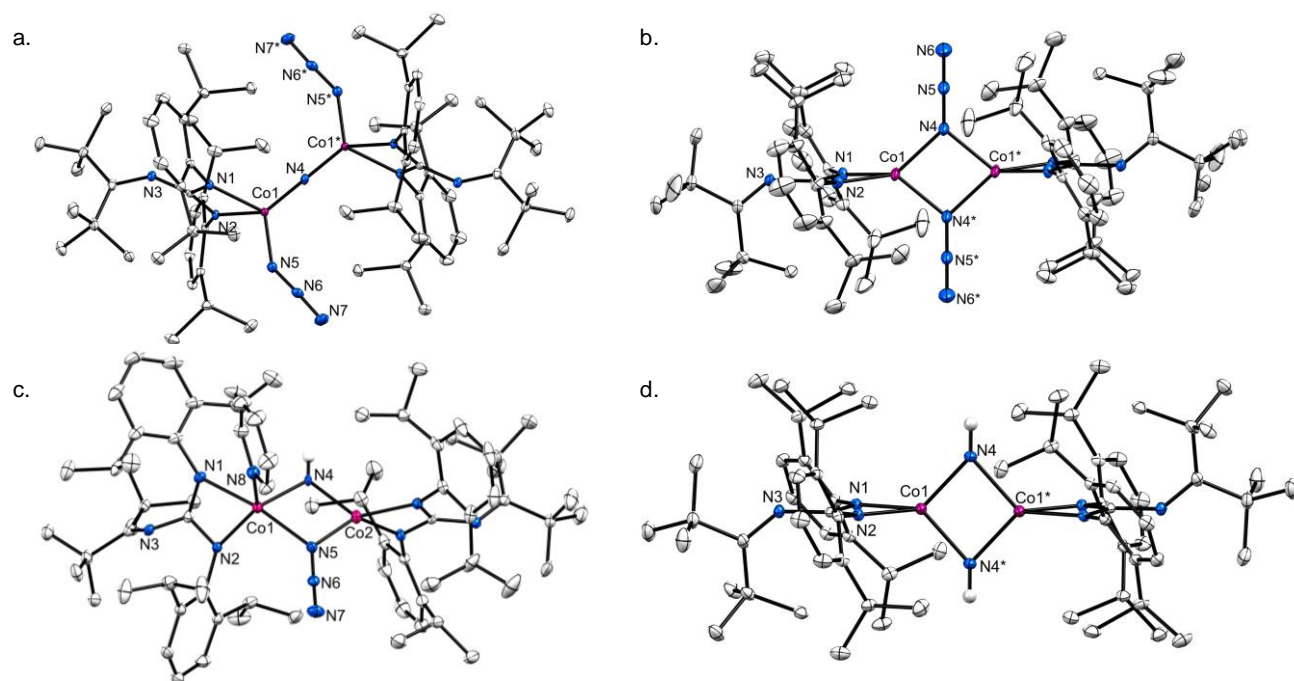


Figure 1. ORTEP representation of compounds (a) **1**·CHD (b) **3b**·THF (c) **5**·C₆H₁₄ and (d) **6**·2C₆H₁₄·2C₅H₁₂ with 30% probability ellipsoids. The [Na(THF)₄]⁺ cation of **1**, the hydrogen atoms (exception N-H of **5** and **6**), and co-crystallized solvents are omitted for clarity. Asterisks denote symmetry generated atoms.

RESULTS AND DISCUSSION

Synthesis and Characterization. Addition of K[(^{ket}guan)] to CoBr₂(DME) in THF affords monomeric (^{ket}guan)Co(Br)(THF) (**2**) which is readily converted to the cobaltate bis(azide) complex [Na(THF)_x][(^{ket}guan)Co(N₃)₂] (**3a**) upon treatment with excess NaN₃ in THF (Scheme 1). Upon dissolution in aromatic or non-polar solvents, the NaN₃ is rapidly lost to give the neutral dimer [(^{ket}guan)Co(N₃)₂]₂ (**3b**) (Scheme 1). As clearly observed through ¹H NMR spectroscopy, **2** – **3** are paramagnetic complexes (Figures S8 – S10). While pristine samples of **3a** are complicated by the facile loss of NaN₃, SQUID magnetometry measurements on solid-state samples of **3b** reveal a room temperature effective magnetic moment of 7.3 μ B (Figure S20). This value is slightly higher than expected for the spin-only value for two non-interacting high spin Co(II) centers (5.48 μ B) but not beyond the range typically encountered for systems with high magnetic anisotropies.^{28–29}

Compound **2** is isolated as a dark blue material, whereas **3a** and **3b** are green solids, all air-sensitive but stable indefinitely under dinitrogen atmosphere. Complex **3a** is primarily stable to NaN₃ loss in THF solution, but typically gives mixtures of **3a** and **3b** upon attempted isolation in the solid state. Regardless, the presence of **3a** in solution is easily detected as it is spectroscopically distinct from **3b** as indicated by NMR and UV-vis spectroscopies.

Single crystals of **3b** can be grown from a saturated THF/hexanes (1:1) solution stored at -30 °C for one day. X-ray diffraction analysis of **3b** confirms the formation of four-coordinate, diamond core cobalt center (Figure 1b). The molecule crystallizes in the *P2₁/c* space group and contains one-half of the dimer in the asymmetric unit which generates the

full molecule through inversion symmetry. The bond metrics of **3b** (Co1–N1 = 1.994(2) Å, Co1–N2 = 1.988(2) Å, Co1–N4 = 1.997(2) Å) are comparable to those found in the related dinuclear cobalt complex {[(ⁱPr₂N)C(NDipp)₂]Co(μ -N₃)}₂ (Co–N = 1.991(3) – 1.994(3) Å, Co–N_{azide} = 2.010(3) Å).³⁰ Inspection of the azide units in **3b** reveals inequivalent N–N distances (N4–N5 = 1.227(3) Å, N5–N6 = 1.135(4) Å) consistent with azide activation,³¹ a feature also present in {[(ⁱPr₂N)C(NDipp)₂]Co(μ -N₃)}₂.

Based upon this observation, attempts were undertaken to initiate N₂ loss to generate cobalt nitrides using **3a** and **3b**. Room temperature photolysis (365 nm) of THF solutions of **3a** gradually gives way to the formation of a new paramagnetic species. The product is sparingly soluble and deposits as a crystalline solid from the photoreaction mixture. Surprisingly, single crystals suitable for X-ray diffraction analysis can be obtained through photolysis of **3a** in THF solution containing excess 1,4-cyclohexadiene (CHD). The solid-state molecular structure revealed the formation of the dinuclear cobalt nitride **1**·CHD (Scheme 1) co-crystallized with a molecule of CHD (Figures 1a and S1).

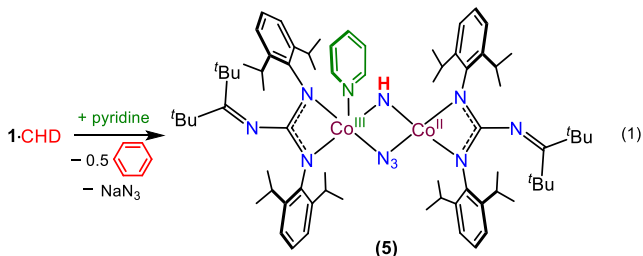
To the best of our knowledge, **1** represents the first example of a low nuclearity cobalt nitride complex as the closest related systems are nitride-encapsulated homo- and heterometallic clusters of the type [Co₁₀Rh(N)₂(CO)₂₁]^{3–32}. Compound **1**·CHD crystallizes in the *P* $\bar{1}$ space group displaying one-half molecule in the asymmetric unit with the full dimer generated through inversion symmetry, and consequently, the Co1–N4–Co1* bond angle is perfectly linear. Examination of the crystallographically unique cobalt-nitride distance (Co1–N4 = 1.678(1) Å) shows that it falls within the typical range of cobalt-imido Co=NR distances (cf.,

$[(^i\text{Pr}_2\text{N})\text{C}(\text{NDipp})_2]\text{Co}(=\text{NAd})$: $\text{Co-N} = 1.621(3)$ Å,³⁰ $[(\text{TIMEN}^{\text{aryl}})\text{Co}(=\text{NAr})](\text{BPh}_4)$: $\text{Co-N} = 1.675(8)$ Å.³³

The metrical parameters of **1** are suggestive of a dimer with a core $\text{Co}=\text{N}=\text{Co}$ unit. Yet, formal charge assignments can be complicated by a number of factors in molecules of this type. For example, the related Rh dimer $(\text{PNN})\text{Rh}(\text{N}\cdot)\text{Rh}(\text{PNN})$ ($\text{PNN} = 6$ -di-*tert*-butylphosphinomethylene-2,2'-bipyridine) is formulated as a Rh(II)/Rh(III) complex with a reactive, bridging nitridyl radical as discerned through electronic structure calculations.³⁴ However, high electron delocalization obfuscates definitive oxidation state assignments, and the rhodium dimer may be more appropriately presented as $\{\text{Rh}_2\text{N}\}^{13}$ utilizing Enemark-Feltham notation. In our case, the room-temperature effective magnetic moment of **1** is $3.60 \mu_{\text{B}}$ (Figure S19). Together with electronic structure analysis (vide infra), the data suggests the presence of two, high-spin Co(III) centers with partial antiferromagnetic coupling giving a total system spin of $S = 2$. Thus, **1** can be formulated as possessing a $\text{Co}^{\text{III}}=\text{N}=\text{Co}^{\text{III}}$ canonical form. In comparison to $\{\text{Rh}_2\text{N}\}^{13}$ in $(\text{PNN})\text{Rh}(\text{N}\cdot)\text{Rh}(\text{PNN})$, **1** contains a $\{\text{Co}_2\text{N}\}^{12}$ unit where the geometry and lower electron count aids in avoiding population of Co-N π^* -orbitals (vide infra).

Betley et al. recently demonstrated that geometric perturbation of the three-coordinate Co(III) imido $(^{\text{dipy}}\text{L})\text{Co}(\text{NR})$ ($^{\text{dipy}}\text{L} = 5$ -mesityl-1,9-(2,4,6- $\text{Ph}_3\text{C}_6\text{H}_2$)dipyrrin) by pyridine ligation to give $(^{\text{dipy}}\text{L})\text{Co}(\text{NR})(\text{py})$ leads to ligand-accelerated C-H bond amination.³⁵ Enhanced reactivity towards C-H bonds in the presence of pyridine with the (salen)ruthenium(VI)-nitrido complex $[(\text{salen})\text{Ru}(\text{N})(\text{MeOH})]\text{PF}_6$ has also been reported.³⁶ In either case, this promotion of reactivity is ascribed in part to the increased electronic saturation at the metal centers after pyridine coordination.

Investigating the role of pyridine coordination in our sys-



tem further, **3a** was treated with a $\text{C}_6\text{H}_6/\text{py}$ (10:1) solution, which produces a mixture of the dimer $[(^{\text{ket}}\text{guan})\text{Co}(\text{N}_3)(\text{py})]_2$ (**4a**) and the 2D-coordination polymer $\{[\text{Na}(\text{THF})_2][(^{\text{ket}}\text{guan})\text{Co}(\text{N}_3)_2]\}_n$ (**4b**) (Figures S4 and S5). Similar solubility properties complicate separation; however, **4a** is selectively obtained from the addition of pyridine to benzene solution of **3b** (Scheme 1). Of further note, the solid-state molecular structure of **4a**·THF· C_5H_{12} (Figure S4) shows azide rearrangement, adopting end-on coordination modes, with the cobalt centers in distorted square pyramidal geometries; yet, poor resolution of the diffraction data only permits a qualitative structural analysis of **4a**·THF· C_5H_{12} , preventing assessment of azide N-N distances and their degree of activation.

Gratifyingly, addition of pyridine to **1**·CHD leads to the quantitative formation of the bimetallic bridging imido **5** where its N-H proton is derived as the product of HAA from the co-crystallized CHD (eq 1). Accordingly, this reaction is accompanied by the formation of 0.5 equiv of benzene (Figure S27). As in the cases of $(^{\text{dipy}}\text{L})\text{Co}(\text{NR})$ and $[(\text{salen})\text{Ru}(\text{N})(\text{MeOH})]\text{PF}_6$, the coordination of pyridine to **1**

acts as a solvent-switch, greatly enhancing the reactivity of the bridging nitride atom.

Furthermore, photolysis of **4a** in $\text{C}_6\text{H}_6/\text{py}$ (10:1) solution also generates **5**; though, when conducted in the absence of H-atom donors such as CHD, the yield is considerably lower and is accompanied by substantial amounts of $^{\text{ket}}\text{guanH}$.

Complex **5** is a dark brown, paramagnetic compound that is soluble in non-polar solvents. Single crystals of **5**· C_6H_{14} are obtained from concentrated hexanes solution, and its solid-state molecular structure (Figure 1c) reveals an asymmetric, bimetallic complex with four- and five-coordinate cobalt centers possessing bridging NH and N_3 groups. The cobalt-imido bond distances of **5**· C_6H_{14} ($\text{Co1-N4} = 1.963(3)$ Å, $\text{Co2-N4} = 1.925(3)$ Å) are not informative as they fall within the range of both amido (cf., $\{[(\text{NH}_2\text{CH}_2\text{CH}_2\text{NH}_2)_2\text{Co}]_2(\mu\text{-NH}_2)(\mu\text{-OH})[\text{NO}_3]_4$: $\text{Co-N} = 1.947(5) - 1.948(5)$ Å³⁷ and imido-bridged cobalt compounds (cf., $\{[\text{HC}(\text{MeCNDipp})]_2\text{Co}(\mu\text{-NAr})_2$: $\text{Co-N} = 1.983(3) - 1.988(3)$ Å).³⁸ On the other hand, SQUID magnetometry measurements of **5** give a room-temperature effective magnetic moment of $3.97 \mu_{\text{B}}$, supportive of a mixed-valent system containing high-spin Co(II) ($S = 1.5$) and low-spin Co(III) ($S = 0$).

Expanding upon the observed pyridine promoted HAA chemistry of **1** towards CHD, its reactivity with other hydrocarbons was studied. Interestingly, addition of pyridine to **1** or photolysis of **4a** in $\text{C}_6\text{H}_6/\text{py}$ in the presence of 9,10-dihydroanthracene (DHA) (BDE: 76.3 kcal/mol)³⁹ fails to give anthracene. We presume this is a consequence of steric hindrance as the two hydrocarbon substrates possess comparably weak C-H bonds (Figure 2a). Notably, $\text{PhB}(\text{BuIm})_3\text{Co}(\text{O})$ is reactive towards DHA, giving $\text{PhB}(\text{BuIm})_3\text{Co}(\text{OH})$ and anthracene as products.²¹

Conversely, **1** is reactive in $\text{C}_6\text{H}_6/\text{py}$ solution towards several hydrocarbon substrates, including those with strong C-H bonds, giving **5** as the sole product in quantitative yields. In particular, HAA is observed with cyclohexene (BDE: 87 kcal/mol) and fully saturated cyclohexane (BDE: 99 kcal/mol) (Figure 2a), yielding benzene in both cases as confirmed by NMR spectroscopy and GC/MS analyses (Figures S30 - S33).³⁹ Interestingly, performing the reaction in the presence of excess cyclooctane (BDE: 95 kcal/mol)³⁹ generates 1,5-cyclooctadiene exclusively (Figures S34 - S36).

The reactivity of our system towards cyclohexane afforded us the opportunity to easily examine the KIE upon switching from C_6H_{12} to C_6D_{12} in the reaction mixtures. Photolysis of **4a** (100 μM) in $\text{C}_6\text{H}_6/\text{py}$ (10:1) in the presence of 100 equiv of cyclohexane was followed by UV-vis absorption spectroscopy (Figure 2b). As seen from the rate plot presented in Figure 2c, there is a clear difference in rate with a $\text{KIE} = 2.5 \pm 0.1$. This value is within the KIE range established for the related Fe=O mediated HAA reactions ($\text{KIE} = 2.5 - 5.7$)⁴⁰ and in complete accordance with the HAA chemistry observed for the $\text{Co}=\text{O}$ complex $[(\text{N4Py})\text{Co}(\text{O})]^{2+}$ ($\text{N4Py} = N,N$ -bis(2-pyridylmethyl)- N -bis(2-pyridyl)methylamine) ($\text{KIE} = 2.1 \pm 0.1$).⁴¹ This reaction can be performed on a preparative scale, giving the isotopomers **5-H** and **5-D** that exhibit imido N-H and N-D stretching frequencies in the infrared spectrum at 3424 cm^{-1} and 2257 cm^{-1} (Figure S17), respectively, within the expected isotopic mass shift range of ca. 2500 cm^{-1} .

Understanding the reactivity of molecular metal nitrides towards hydrogen is very important for providing chemical insights into the formation of ammonia through the Haber-Bosch process.⁴² Despite this, only a few examples of nitride

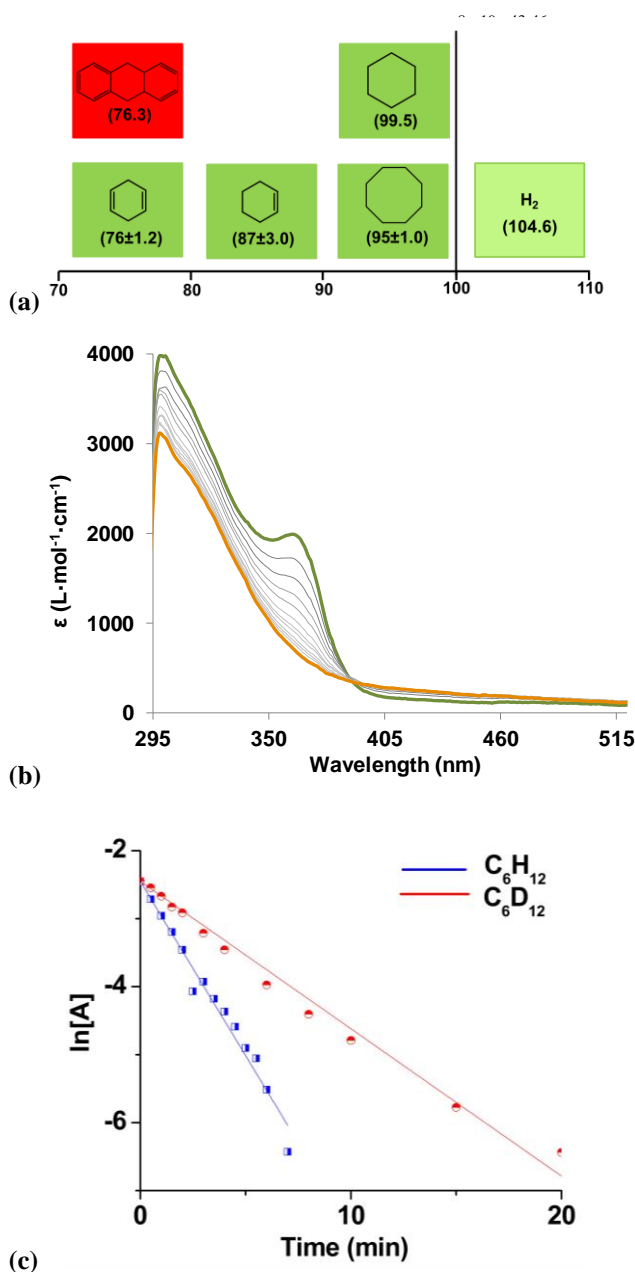


Figure 2. (a) Substrate screening for the HAA chemistry of **1** and respective C-H BDEs. (b) UV-vis spectra of the photoconversion of **4a** (green) to **5** (orange) in C₆H₆/py solution in the presence of excess CHD. (c) KIE rate plot of the photolysis of **4a** in C₆H₆/py (10:1) in the presence of 100 equiv of C₆H₁₂ (blue) and C₆D₁₂ (red).

Whether **6** forms from the heterolytic or homolytic cleavage of H₂ is not known at this time, though the preference in our system for HAA of strong C-H bonds suggests the latter. Conducting the experiment in C₆D₆/py-*d*₅ with H₂ exclusively gives **6-H** with a N-H stretching frequency appearing at 3422 cm⁻¹ (Figure S18), indicating no HAA reactivity with the solvent. Moreover, photolyzing C₆D₆/py-*d*₅ solutions of **5** under H₂ (150 psi) gradually gives way to **6**, suggesting the formation of the bis(imido) occurs stepwise.

Computed Geometry and Electronic Structure. To scrutinize the electronic structure of **1**, we turned to density functional theory (DFT). Using a non-truncated model of **1**, in an

anionic form without the [Na(THF)₄]⁺ counterion, the empirical X-ray structure was remarkably reproduced by dispersion-corrected DFT calculations in the quintet spin state (see Supporting Information for details). We used quasi-restricted orbitals (QROs) (Figure 3) to rationalize and characterize the electronic structure of **1**. QROs express unrestricted wavefunctions (with different α and β orbital subsets) through the intuitive conceptual picture of the restricted open-shell (RO) solution with doubly and singly occupied orbitals (i.e. through identical α and β spatial orbitals).

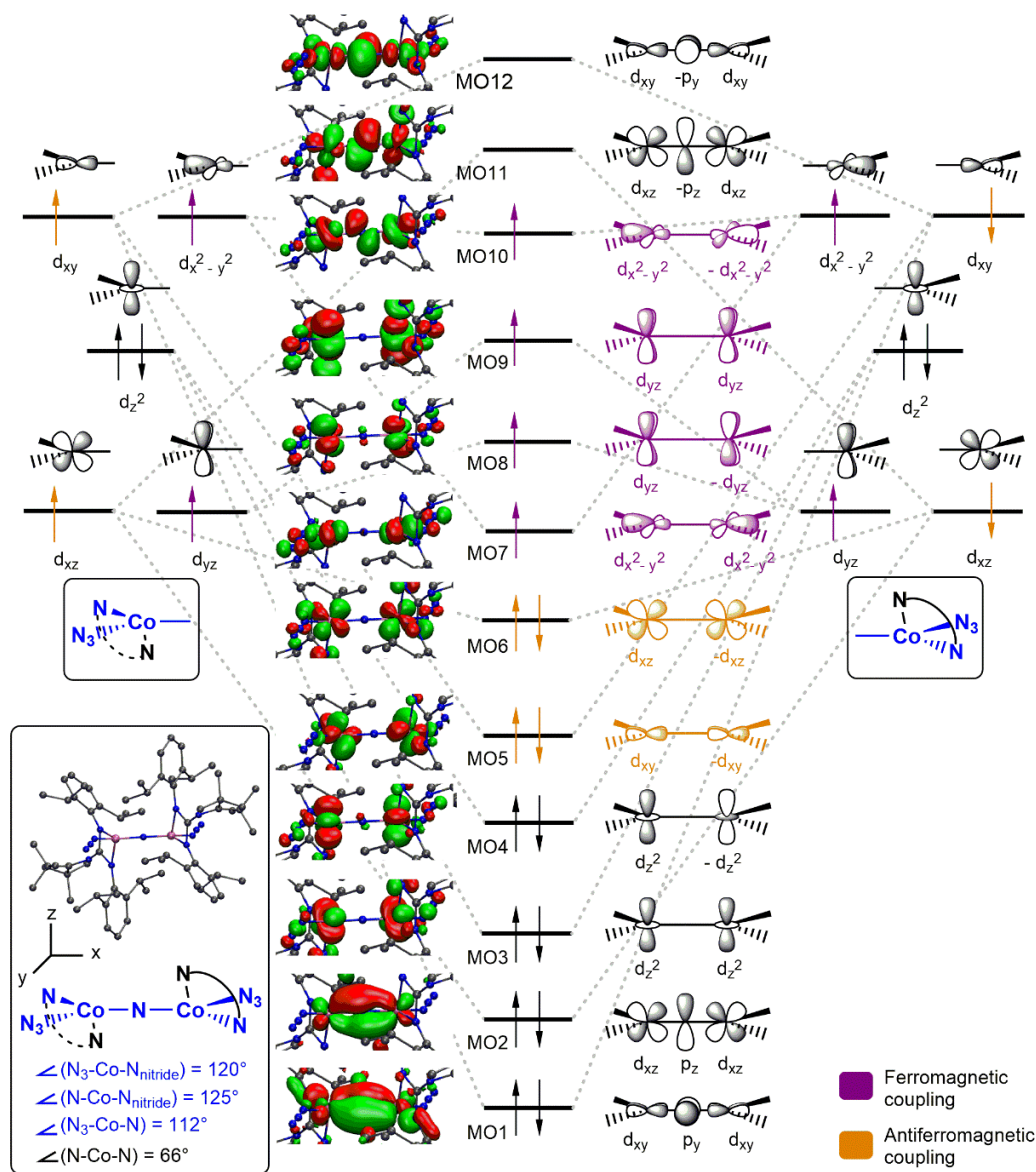


Figure 3. Molecular orbital diagram of the Co-N-Co core of **1**.

According to the features of the revealed molecular QROs, **1** can be formally described as possessing two, high-spin Co(III) centers exhibiting both antiferromagnetic and weak ferromagnetic coupling through two two-electron interactions each (Figure 3). The formal partition of these delocalized MOs to individual cobalt contributions gives four half-filled d-orbitals, d_{xz} , d_{yz} , d_{xy} , and $d_{x^2-y^2}$ with a doubly occupied d_{z^2} -orbital at each metal. At each cobalt, two of the metal-centered radicals couple antiferromagnetically in the p-subspace mediated by the bridging nitride, whereas the couplings of unpaired electrons with local s- and d-symmetries through the nitrogen are limited and, accordingly, remain weak and ferromagnetic in nature. This gives an overall quintet spin-state, which agrees with the measured effective magnetic moment of $3.60 \mu_B$, substantiating the model and chosen analysis method. A similar magnetic phenomenon has been documented in the case of $[(NNNO)Ni(\mu-N_3)]_2$, which also exhibits both antiferromagnetic and ferromagnetic coupling interactions.⁴⁷

To better envisage the bonding interactions in **1**, a simplified substructure of the “(ket^guan)Co(μ -N)(N₃)” unit can be

defined by the cobalt center, its azide group, the bridging N_{nitride}, and one of the nitrogen contact atoms from each [ket^guan][−] ligand, giving an ML₃ structural approximation for each metal which is highlighted in blue in Figure 3 (see inset). This yields a planar arrangement where the ligand atoms are separated by nearly 120°, affording a D_{3h} symmetry approximation for each cobalt fragment with the out-of-plane nitrogen atom of the [ket^guan][−] ligand acting as an asymmetric axial perturbation on the idealized electronic structure at the metal. Through this perspective, the d-orbital arrangement represents the most ideal orientation for the schematic representation of the cobalt-nitride and cobalt-cobalt interactions.

Accordingly, the in-plane d_{xy} orbitals are perfectly oriented on both sides to form an appreciable three-center, two-electron overlap integral with the p_y orbital of the N_{nitride} atom as seen in the molecular orbital picture, MO1, in Figure 3. An almost identical three-center π -interaction (MO2) evolves in the perpendicular xz-plane through the Co(d_{xz})+N(p_z)+Co(d_{xz}) atomic orbital combination. Both of these molecular orbitals formally represent N_{nitride}-based lone pairs; however, the spatial distri-

butions clearly expose delocalization to the metals resulting in the formation of π -type bonding interactions of covalent character. The two other lone pairs of the formally N^{-3} bridge are represented by low lying orbitals with $N(p_x)$ and $N(s)$ character (not shown in Figure 3).

These three-center, two-electron combinations give way to the $d_{xy}-d_{xy}$ (MO5) and $d_{xz}-d_{xz}$ (MO6), antisymmetric nonbonding orbital configurations (Figure 3), leading to antiferromagnetic coupling of the metal-centered electrons in non-degenerate molecular orbitals. In contrast, the symmetric and antisymmetric σ - and δ -symmetry oriented d-orbitals, $d_{x^2-y^2}-d_{x^2-y^2}$ and $d_{yz}-d_{yz}$, respectively, appear as quasi-degenerate orbitals (MO7 – MO10) with each hosting one electron according to Hund's maximum multiplicity rule.

Owing to the strong delocalization of the nitride lone-pairs to the metals (MO1 and MO2), the central Co-N interactions have a notable π -bond character in addition to the dative σ -bond. Accordingly, the electronic structure of **1** can be best represented by the $Co^{III}=N=Co^{III}$ canonical form, with the data indicating no radical character at the nitride atom. Mayer bond orders of 1.33 calculated for the Co-N interactions support this notion. The spin density value of 1.5 at each cobalt conforms also to the deduced electronic structure with partial antiferromagnetic coupling. As the unpaired electrons occupy σ - and δ -symmetry metal orbitals that cannot mix with the nitrogen's π -symmetry p_x and p_z atomic orbitals, the radical character cannot delocalize to the bridging nitrogen, which is reflected by the negligible atom-condensed spin density value of 0.1 at the nitrogen.

The lowest-lying unoccupied molecular orbitals, MO11 and MO12, correspond to the antibonding combinations of the $Co=N=Co$ π -interactions and have notable amplitude at the central nitrogen due to the covalent nature of the Co-N π -bonds. In comparison, the reported spin density distribution of the related dimer $(PNN)Rh(N\cdot)Rh(PNN)^{15}$ closely resembles the out of plane antibonding combination of **1**, MO11, with one electron occupancy of this orbital in the dirhodium nitride case. As a matter of fact, this additional electron within the $\{Rh_2N\}^{13}$ core of $(PNN)Rh(N\cdot)Rh(PNN)$ embodies the most significant formal difference between its electronic structure and the $\{Co_2N\}^{12}$ core of **1**, thus giving way to the observed nitridyl radical character in $(PNN)Rh(N\cdot)Rh(PNN)$ that is absent in **1**.

CONCLUSION

In conclusion, while late metal complexes of the type $M=E/M\equiv E$ can be difficult to access and stabilize owing to "oxo wall" considerations, we show here that surrogates for such chemistry can be obtained through systems of the type $M=E=M$. In this case, we demonstrate that the first example of a bimetallic cobalt nitride, compound **1**, is easily accessed through photolysis of a guanidinate cobalt-azide precursor. According to DFT calculations, conforming also to experimental observations, **1** possesses two high-spin cobalt(III) centers coupled through a formal $Co^{III}=N=Co^{III}$ core with covalent Co-N π -bonds. The pseudo-planar arrangement about the $Co^{III}=N=Co^{III}$ unit facilitates the antiferromagnetic coupling of π -symmetry metal-centered radicals (two at each Co) across the bridging nitride, whereas the inefficient through-space interaction of σ - and δ -symmetry d-orbitals leads to the weak ferromagnetic coupling of the corresponding unpaired electrons (also two at each Co), eventuating in an S=2, quintet

spin-state of **1**. The geometry and electron count of the cobalt centers avoids population of Co-N π^* -orbitals, thereby avoiding radical character at the N-atom. Consequently, **1** is stable in solution and as a solid. However, its N-atom reactivity is accessible through addition of pyridine, triggering HAA chemistry to give the bridged imido **5**. Impressively, this HAA reactivity extends to strong C-H bonds such as those found in cyclohexane (BDE ~ 100 kcal/mol). Moreover, this chemistry can be further extended to include H_2 , leading to a rare example of hydrogen activation by a molecular metal nitride to generate the bis(imido) **6**. At present, investigations are underway to understand the observed H_2 activation chemistry while working to apply our synthetic strategy to other late metal systems.

ASSOCIATED CONTENT

Supporting Information

The Supporting Information is available free of charge on the ACS Publications website. Crystallographic details (CIF) and the supporting Information is available free of charge on the ACS Publication Website at DOI:

Experimental procedures, spectral data for all the complexes, magnetic data and computational details (PDF)

AUTHOR INFORMATION

Corresponding Authors

*asfortier@utep.edu,

*balazs.pinter@usm.cl

ORCID

Debabrata Sengupta: 0000-0001-7212-3761

Ram Seshadri: 0000-0001-5858-4027

Balazs Pinter: 0000-0002-0051-5229

Skye Fortier: 0000-0002-0502-5229

Notes

The authors declare no competing financial interests.

ACKNOWLEDGMENT

We are grateful to the NSF (CHE-1664938 and DMR-1827745; S.F.) and the Welch Foundation (AH-1922-20170325; S.F) for financial support of this work. S.F. is an Alfred P. Sloan Foundation research fellow and is thankful for their support. We also wish to acknowledge the NSF-MRI program (CHE-1827875) for providing funding for the purchase of an X-ray diffractometer. Magnetic measurements were performed at the shared experimental facilities of the NSF Materials Research Science and Engineering Center (MRSEC) at UC Santa Barbara (DMR 1720256). The UCSB MRSEC is a member of the NSF-supported Materials Research Facilities Network (www.mrfrn.org).

REFERENCES

- (1) Hohenberger, J.; Ray, K.; Meyer, K., The biology and chemistry of high-valent iron-oxo and iron-nitrido complexes. *Nat. Commun.* **2012**, 3, 720.
- (2) *Handbook of Metathesis*. Wiley-VCH Verlag GmbH & Co: 2015.
- (3) Schrock, R. R., Multiple metal-carbon bonds for catalytic metathesis reactions (Nobel Lecture). *Angew. Chem. Int. Ed.* **2006**, 45, 3748-3759.

- (4) Smith, J. M., Reactive transition metal nitride complexes. *Prog. Inorg. Chem.* **2014**, *58*, 417-470.
- (5) Gray, H. B.; Winkler, J. R., Living with Oxygen. *Acc. Chem. Res.* **2018**, *51*, 1850-1857.
- (6) Berry, J. F., Terminal nitrido and imido complexes of the late transition metals. *Comments Inorg. Chem.* **2009**, *30*, 28-66.
- (7) Hartmann, N. J.; Wu, G.; Hayton, T. W., Synthesis of a "Masked" Terminal Nickel(II) Sulfide by Reductive Deprotection and its Reaction with Nitrous Oxide. *Angew. Chem. Int. Ed.* **2015**, *54*, 14956-14959.
- (8) Scheibel, M. G.; Askevold, B.; Heinemann, F. W.; Reijerse, E. J.; de Bruin, B.; Schneider, S., Closed-shell and open-shell square-planar iridium nitrido complexes. *Nat. Chem.* **2012**, *4*, 552-558.
- (9) O'Halloran, K. P.; Zhao, C. C.; Ando, N. S.; Schultz, A. J.; Koetzle, T. F.; Piccoli, P. M. B.; Hedman, B.; Hodgson, K. O.; Bobyr, E.; Kirk, M. L.; Knottenbelt, S.; Depperman, E. C.; Stein, B.; Anderson, T. M.; Cao, R.; Geletii, Y. V.; Hardcastle, K. I.; Musaev, D. G.; Neiwert, W. A.; Fang, X. K.; Morokuma, K.; Wu, S. X.; Kogerler, P.; Hill, C. L., Revisiting the Polyoxometalate-Based Late-Transition-Metal-Oxo Complexes: The "Oxo Wall" Stands. *Inorg. Chem.* **2012**, *51*, 7025-7031.
- (10) Winkler, J. R.; Gray, H. B., Electronic structures of oxo-metal ions. *Struct. Bonding (Berlin, Ger.)* **2012**, *142* (Molecular Electronic Structures of Transition Metal Complexes I), 17-28.
- (11) Schoffel, J.; Susnjar, N.; Nuckel, S.; Sieh, D.; Burger, P., 4d vs. 5d-Reactivity and Fate of Terminal Nitrido Complexes of Rhodium and Iridium. *Eur. J. Inorg. Chem.* **2010**, 4911-4915.
- (12) Rebreyend, C.; Mouarrawis, V.; Siegler, M. A.; van der Vlugt, J. I.; de Bruin, B., Steric Protection of Rhodium-Nitridyl Radical Species. *Eur. J. Inorg. Chem.* **2019**, 4249-4255.
- (13) Saouma, C. T.; Peters, J. C., M E and M=E complexes of iron and cobalt that emphasize three-fold symmetry (E O, N, NR). *Coord. Chem. Rev.* **2011**, *255*, 920-937.
- (14) Hay-Motherwell, R. S.; Wilkinson, G.; Hussain-Bates, B.; Hursthouse, M. B., Synthesis and x-ray crystal structure of oxotrimesityliridium(V). *Polyhedron* **1993**, *12*, 2009-12.
- (15) Gloaguen, Y.; Rebreyend, C.; Lutz, M.; Kumar, P.; Huber, M.; van der Vlugt, J. I.; Schneider, S.; de Bruin, B., An Isolated Nitridyl Radical-Bridged {Rh(N)Rh} Complex. *Angew. Chem. Int. Ed.* **2014**, *53*, 6814-6818.
- (16) Scheibel, M. G.; Wu, Y.; Stueckl, A. C.; Krause, L.; Carl, E.; Stalke, D.; de Bruin, B.; Schneider, S., Synthesis and Reactivity of a Transient, Terminal Nitrido Complex of Rhodium. *J. Am. Chem. Soc.* **2013**, *135*, 17719-17722.
- (17) Angersbach-Bludau, F.; Schulz, C.; Schoeffel, J.; Burger, P., Syntheses and electronic structures of μ -nitrido bridged pyridine, diimine iridium complexes. *Chem. Commun. (Cambridge, U. K.)* **2014**, *50*, 8735-8738.
- (18) Schoeffel, J.; Rogachev, A. Y.; DeBeer George, S.; Burger, P., Isolation and Hydrogenation of a Complex with a Terminal Iridium-Nitrido Bond. *Angew. Chem. Int. Ed.* **2009**, *48*, 4734-4738.
- (19) Schoffel, J.; Rogachev, A. Y.; George, S. D.; Burger, P., Isolation and Hydrogenation of a Complex with a Terminal Iridium-Nitrido Bond. *Angew. Chem. Int. Ed.* **2009**, *48*, 4734-4738.
- (20) Sieh, D.; Schlimm, M.; Andernach, L.; Angersbach, F.; Nuckel, S.; Schoffel, J.; Susnjar, N.; Burger, P., Metal-Ligand Electron Transfer in 4d and 5d Group 9 Transition Metal Complexes with Pyridine, Diimine Ligands. *Eur. J. Inorg. Chem.* **2012**, 444-462.
- (21) Goetz, M. K.; Hill, E. A.; Filatov, A. S.; Anderson, J. S., Isolation of a Terminal Co(III)-Oxo Complex. *J. Am. Chem. Soc.* **2018**, *140*, 13176-13180.
- (22) Hojilla Atienza, C. C.; Bowman, A. C.; Lobkovsky, E.; Chirik, P. J., Photolysis and Thermolysis of Bis(imino)pyridine Cobalt Azides: C-H Activation from Putative Cobalt Nitrido Complexes. *J. Am. Chem. Soc.* **2010**, *132* (46), 16343-16345.
- (23) Zolnhofer, E. M.; Kaess, M.; Khusniyarov, M. M.; Heinemann, F. W.; Maron, L.; van Gastel, M.; Bill, E.; Meyer, K., An Intermediate Cobalt(IV) Nitrido Complex and its N-Migratory Insertion Product. *J. Am. Chem. Soc.* **2014**, *136*, 15072-15078.
- (24) Pfaff, F. F.; Kundu, S.; Risch, M.; Pandian, S.; Heims, F.; Pryjomska-Ray, I.; Haack, P.; Metzinger, R.; Bill, E.; Dau, H.; Comba, P.; Ray, K., An Oxocobalt(IV) Complex Stabilized by Lewis Acid Interactions with Scandium(III) Ions. *Angew. Chem. Int. Ed.* **2011**, *50*, 1711-1715.
- (25) Cui, P.; Wang, Q.; McCollom, S. P.; Manor, B. C.; Carroll, P. J.; Tomson, N. C., Ring-Size-Modulated Reactivity of Putative Dicobalt-Bridging Nitrides: C-H Activation versus Phosphinimide Formation. *Angew. Chem. Int. Ed.* **2017**, *56*, 15979-15983.
- (26) Maity, A. K.; Metta-Magana, A. J.; Fortier, S., Donor Properties of a New Class of Guanidinate Ligands Possessing Ketimine Backbones: A Comparative Study Using Iron. *Inorg. Chem.* **2015**, *54*, 10030-10041.
- (27) Maity, A. K.; Murillo, J.; Metta-Magana, A. J.; Pinter, B.; Fortier, S., A Terminal Iron(IV) Nitride Supported by a Super Bulky Guanidinate Ligand and Examination of Its Electronic Structure and Reactivity. *J. Am. Chem. Soc.* **2017**, *139*, 15691-15700.
- (28) Fortier, S.; Le Roy, J. J.; Chen, C. H.; Vieru, V.; Murugesu, M.; Chibotaru, L. F.; Mindiola, D. J.; Caulton, K. G., A Dinuclear Cobalt Complex Featuring Unprecedented Anodic and Cathodic Redox Switches for Single-Molecule Magnet Activity. *J. Am. Chem. Soc.* **2013**, *135*, 14670-14678.
- (29) Fortier, S.; Moral, O. G. D.; Chen, C. H.; Pink, M.; Le Roy, J. J.; Murugesu, M.; Mindiola, D. J.; Caulton, K. G., Probing the redox non-innocence of dinuclear, three-coordinate Co(II) nindigo complexes: not simply beta-diketiminato variants. *Chem. Commun.* **2012**, *48*, 11082-11084.
- (30) Jones, C.; Schulten, C.; Rose, R. P.; Stasch, A.; Aldridge, S.; Woodul, W. D.; Murray, K. S.; Moubaraki, B.; Brynda, M.; La Macchia, G.; Gagliardi, L., Amidinato- and Guanidinato-Cobalt(I) Complexes: Characterization of Exceptionally Short Co-Co Interactions. *Angew. Chem. Int. Ed.* **2009**, *48*, 7406-7410.
- (31) Torniepothoetting, I. C.; Klapotke, T. M., Covalent Inorganic Azides. *Angew. Chem. Int. Ed.* **1995**, *34*, 511-520.
- (32) Costa, M.; Della Pergola, R.; Fumagalli, A.; Laschi, F.; Losi, S.; Macchi, P.; Sironi, A.; Zanella, P., Mixed Co-Rh nitrido-encapsulated carbonyl clusters. Synthesis, solid-state structure, and electrochemical/EPR characterization of the anions $[\text{Co}_{10}\text{Rh}(\text{N})_2(\text{CO})_{21}]^{3-}$, $[\text{Co}_{10}\text{Rh}_2(\text{N})_2(\text{CO})_{24}]^{2-}$, and $[\text{Co}_{11}\text{Rh}(\text{N})_2(\text{CO})_{24}]^{2-}$. *Inorg. Chem.* **2007**, *46*, 552-560.
- (33) Hu, X. L.; Meyer, K., Terminal cobalt(III) imido complexes supported by tris(carbene) ligands: Imido insertion into the cobalt-carbene bond. *J. Am. Chem. Soc.* **2004**, *126*, 16322-16323.
- (34) Gloaguen, Y.; Rebreyend, C.; Lutz, M.; Kumar, P.; Huber, M.; van der Vlugt, J. I.; Schneider, S.; de Bruin, B., An Isolated Nitridyl Radical-Bridged {Rh(N-center dot)Rh} Complex. *Angew. Chem. Int. Ed.* **2014**, *53*, 6814-6818.
- (35) Baek, Y.; Betley, T. A., Catalytic C-H Amination Mediated by Dipyrrin Cobalt Imidos. *J. Am. Chem. Soc.* **2019**, *141*, 7797-7806.
- (36) Man, W. L.; Lam, W. W. Y.; Kwong, H. K.; Yiu, S. M.; Lau, T. C., Ligand-Accelerated Activation of Strong C-H Bonds of Alkanes by a (Salen)ruthenium(VI)-Nitrido Complex. *Angew. Chem. Int. Ed.* **2012**, *51*, 9101-9104.
- (37) Marsh, R. E.; Thewalt, U., Structure of racemic .mu.-amido-.mu.-hydroxy-bis[bis(ethylenediamine)cobalt(III)] tetranitrate hydrate. *Inorg. Chem.* **1971**, *10*, 1789-1795.
- (38) Dai, X. L.; Kapoor, P.; Warren, T. H., $[\text{Me}_2\text{NN}]\text{Co}(\eta^6\text{-toluene})$: O = O, N = N, and O = N bond cleavage provides, beta-diketiminato cobalt mu-oxo and imido complexes. *J. Am. Chem. Soc.* **2004**, *126*, 4798-4799.
- (39) Xue, X.-S.; Ji, P.; Zhou, B.; Cheng, J.-P., The Essential Role of Bond Energetics in C-H Activation/Functionalization. *Chem. Rev. (Washington, DC, U. S.)* **2017**, *117*, 8622-8648.
- (40) Andris, E.; Navratil, R.; Jasik, J.; Thibault, T.; Srnc, M.; Costas, M.; Roithova, J., Chasing the Evasive Fe=O Stretch and the Spin State of the Iron(IV)-Oxo Complexes by Photodissociation Spectroscopy. *J. Am. Chem. Soc.* **2017**, *139*, 2757-2765.
- (41) Andris, E.; Navratil, R.; Jasik, J.; Srnc, M.; Rodriguez, M.; Costas, M.; Roithova, J., M-O Bonding Beyond the Oxo Wall: Spectroscopy and Reactivity of Cobalt(III)-Oxyl and Cobalt(III)-Oxo Complexes. *Angew. Chem. Int. Ed.* **2019**, *58*, 9619-9624.
- (42) Holscher, M.; Leitner, W., Catalytic NH₃ Synthesis using N-2/H-2 at Molecular Transition Metal Complexes: Concepts for Lead

Structure Determination using Computational Chemistry. *Chem-Eur. J.* **2017**, 23, 11992-12003.

(43) Brown, S. D.; Mehn, M. P.; Peters, J. C., Heterolytic H-2 activation mediated by low-coordinate $L_3Fe-(\mu-N)-FeL_3$ complexes to generate $Fe(\mu-NH)(\mu-H)Fe$ species. *J. Am. Chem. Soc.* **2005**, 127, 13146-13147.

(44) Askevold, B.; Nieto, J. T.; Tussupbayev, S.; Diefenbach, M.; Herdtweck, E.; Holthausen, M. C.; Schneider, S., Ammonia formation by metal-ligand cooperative hydrogenolysis of a nitrido ligand. *Nat. Chem.* **2011**, 3, 532-537.

(45) Schendzielorz, F. S.; Finger, M.; Volkmann, C.; Wurtele, C.; Schneider, S., A Terminal Osmium(IV) Nitride: Ammonia Formation and Ambiphilic Reactivity. *Angew. Chem. Int. Ed.* **2016**, 55, 11417-11420.

(46) Falcone, M.; Poon, L. N.; Tirani, F. F.; Mazzanti, M., Reversible Dihydrogen Activation and Hydride Transfer by a Uranium Nitride Complex. *Angew. Chem. Int. Ed.* **2018**, 57, 3697-3700.

(47) Sarkar, S.; Datta, A.; Mondal, A.; Chopra, D.; Ribas, J.; Rajak, K. K.; Sairam, S. M.; Pati, S. K., Competing Magnetic Interactions in a Dinuclear Ni(II) Complex: Antiferromagnetic O-H...O Moiety and Ferromagnetic N3- Ligand. *J. Phys. Chem. B* **2006**, 110, 12-15.
